Scripta Materialia 234 (2023) 115565

Contents lists available at ScienceDirect

Scripta Materialia

journal homepage: www.journals.elsevier.com/scripta-materialia

Role of Aluminum rejection from isothermal ω precipitates on the formation of α precipitates in the metastable β-titanium alloy Ti-10V-2Fe-3Al

S.A. Mantri [a,*,1], S. Dasari [a], A. Sharma [a], Y. Zheng [b], H.L. Fraser [c], R. Banerjee [a,*]

[a] Department of Materials Science and Engineering, University of North Texas, Denton, Texas 76207, USA
[b] Department of Chemical and Materials Engineering, University of Nevada Reno, Reno, NV 89557, USA
[c] Center for the Accelerated Maturation of Materials, Department of Materials Science and Engineering, The Ohio State University, 1305 Kinnear Road, Columbus, OH 43212, USA, of North Texas, Denton, TX, USA

ARTICLE INFO

Keywords:
beta titanium alloys
phase transformations
atom probe tomography
α precipitation

ABSTRACT

The formation of isothermal ω phase precipitates and its influence on subsequent fine-scale α precipitation is investigated in a metastable β-titanium alloy, Ti-10V-2Fe-3Al. Atom-probe tomography and high-resolution transmission electron microscopy reveal that the rejection of Al, a potent α stabilizer, from the growing isothermal ω precipitates at 330°C, aids in the formation of α precipitates. Additionally, the presence of α/ω and α/β interfaces conclusively establish that these α precipitates form at the β/ω interface. Interestingly, the local Al pile-up at this interface results in a substantially higher than equilibrium Al content within the α precipitates at the early stages of formation. This can be rationalized based on a novel three-phase β+ω+α metastable equilibrium at a lower annealing temperature (330°C, below the ω solvus). Subsequent annealing at a higher temperature (600°C, above the ω solvus), dissolves the ω precipitates and re-establishes the two-phase β+α equilibrium in concurrence with solution thermodynamic predictions.

The last few years have seen a substantial increase in studies focused on the mechanisms underlying fine-scale α (HCP) precipitation in the BCC matrix of β-titanium alloys [1–5]. This increased interest can be attributed to the ability of tuning the microstructures and achieve exceptional mechanical properties in these alloys [6–8]. By controlling the volume fraction, size distribution, and morphology of the fine-scale α precipitates, it is possible to achieve a wide range of strength-ductility combinations [8–10]. The metastable ω phase has been reported to play an important role on fine scale α precipitation in these β-Ti alloys. ω can form athermally when quenched from the β phase purely via displacive atomic shuffling [11]. Upon aging at low temperatures, isothermal ω precipitates are formed via a diffusion-mediated process [12–14]. The subject of ω assisted α nucleation in these alloys has attracted a lot of recent attention, with multiple research groups focusing on developing a clear understanding of the role of ω on fine scale α precipitation. Multiple factors have been proposed, including, the β/ω interface acting as heterogeneous α nucleation sites [1,5], the coherency stresses arising due to the β/ω misfit, the enhanced chemical driving force for α precipitation near ω precipitates due to local rejection of β stabilizers [15,16], and the influence of local oxygen enrichment in the vicinity of ω precipitates increasing the driving force for α precipitation [2,3,17]. Additionally, in β-Ti alloys containing Al (a potent α stabilizer), such as Ti-6.8Mo-4.5Fe-1.5Al [15] and Ti-5Al-5V-5Mo-3Cr (or Ti-5553) [1], it was proposed that the α precipitates nucleate in the vicinity of ω/β interfaces, due to local Al enrichment (rejection from the isothermal ω precipitates). However, there was no conclusive evidence regarding the proposed compositional enrichment of Al, presented in these papers and there was a controversy regarding whether these α precipitates formed at the ω/β interface or at a distance from the interface. However, the more recent atomic resolution HAADF-STEM results from aberration-corrected TEM carried out on ω-assisted α precipitation in Ti-5553 by Zheng et. al.[18–20], clearly established that the α precipitates shared common interfaces with the adjacent ω precipitates and the β matrix. The present work investigates the role of ω precipitates on fine scale α precipitation in a commercial metastable β alloy, Ti-10V-2Fe-3Al (or Ti-10-2-3), with a focus on clearly establishing

* Corresponding authors.
E-mail addresses: mantrisa@anl.gov (S.A. Mantri), raj.banerjee@unt.edu (R. Banerjee).
[1] Present address: Argonne National Laboratory, Lemont, IL 60439, USA.

https://doi.org/10.1016/j.scriptamat.2023.115565
Received 12 April 2023; Received in revised form 4 May 2023; Accepted 12 May 2023
Available online 16 May 2023

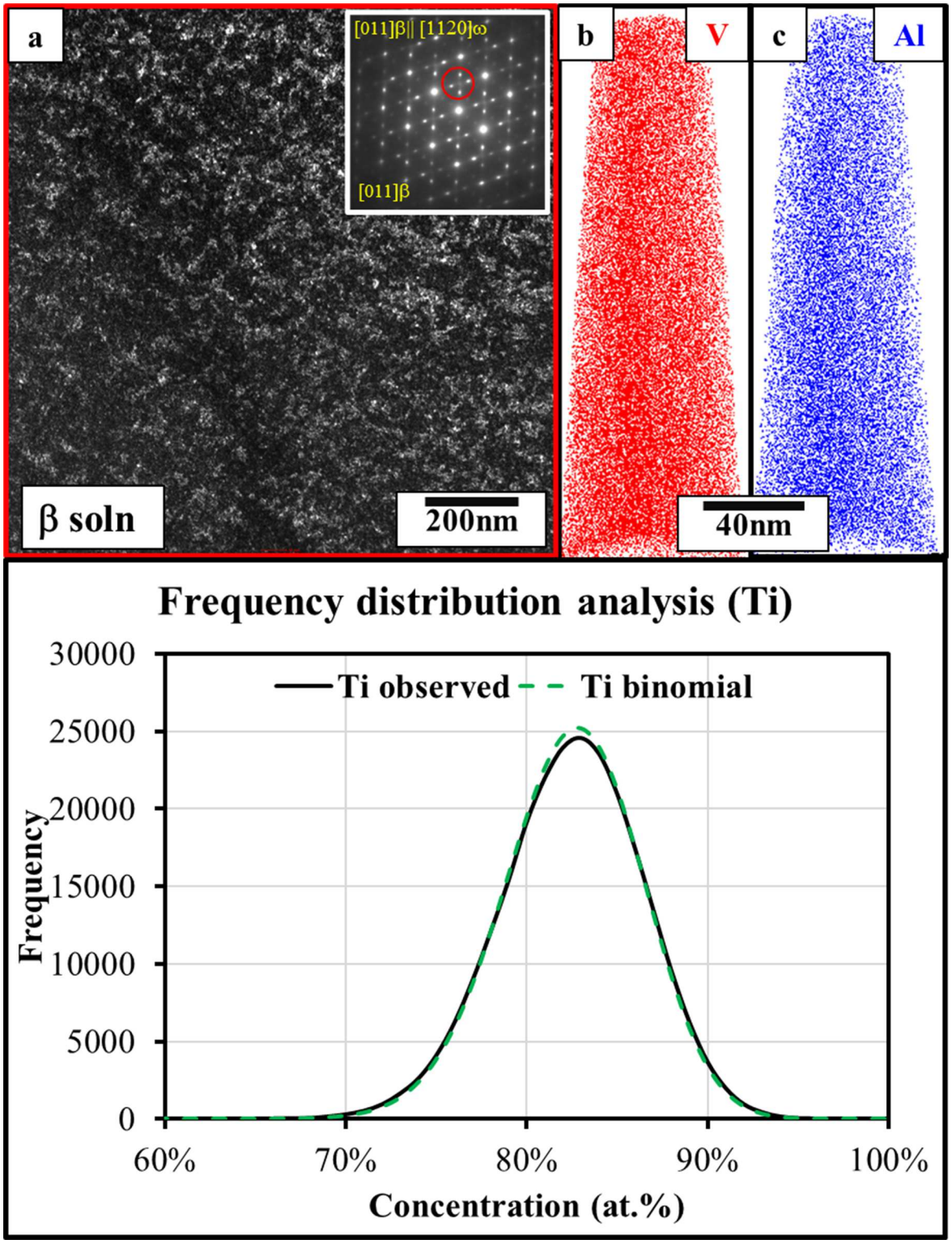

Fig. 1. β solutionized sample: (a) DFTEM image recorded along [110]β, shown as an inset (c) elemental maps of the major elements do not show any partitioning, further collaborated by frequency distribution analysis (Ti)

the role of Al. Preliminary work on phase transformations in the Ti-10-2-3 alloy was performed by Duerig et al [21]. This study rationalized that since Ti-10-2-3 contains both vanadium (high β/ω misfit) and iron (low β/ω misfit), the ω phase formed, depending on the aging treatment, can be either cuboidal or ellipsoidal. At lower annealing temperatures and times, the ω phase formed is ellipsoidal in nature and with an increase in annealing time, leading to increased out diffusion of the β stabilizers (V, Fe), the morphology of the ω precipitates changes to cuboids. These previous studies lay the perfect background motivating the present investigation on the influence of precursory ω precipitates on fine scale α precipitation in the Ti-10-2-3 alloy.

Bars of Ti-10V-2Fe-3Al (in wt. %) were provided by ATI Company. All specimens were first solutionized at 900°C for 30 min followed by water quenching. Following this, the specimens were then subjected to

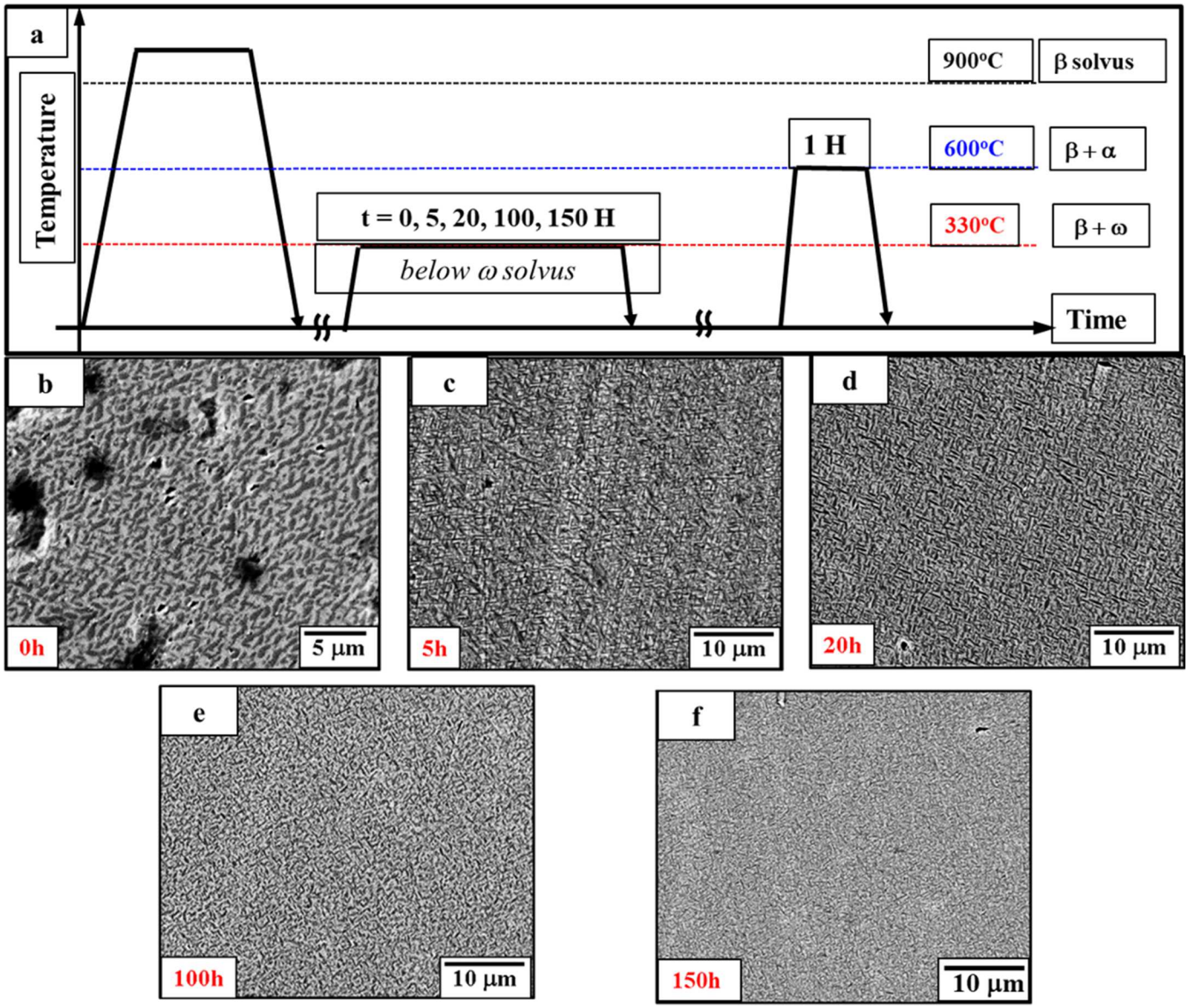

Fig. 2. (a) Schematic showing the heat treatment for the fine scale α precipitation; (b–f) backscattered scanning electron images showing the α precipitates at different aging periods from 0H to 150H.

isothermal annealing at 330°C for periods ranging from 0H to 150H, to vary the ω volume fraction. Subsequently, specimens were annealed within the α+β phase field at 600°C for 1H to promote α precipitation [22]. The schematic of all these heat treatments is shown in Fig. 2(a). Microstructural characterization was carried out in a FEI NovaNano SEM230 and a FEI Tecnai F20-FEG TEM operated at 200 kV. Phase compositions were extracted using a 3D atom probe tomography (APT) in a LEAP™ system from Cameca Inc. For both TEM and APT analysis, samples were prepared using a dual-beam FIB-Nova Nanolab 200 system from FEI. It is to be noted that while the alloy composition (Ti-10V-2-Fe-3Al) is in wt. %, all the results obtained via APT are presented in at. %. Thermodynamic calculations were generated using Pandat software [23].

Since the SEM images showed only single β grains in the samples after β-solutionizing, further detailed TEM analysis was warranted. A representative dark-field TEM (DFTEM) recorded along the <011>β zone axis is shown in Fig. 1(a) with the corresponding <011>β zone axis selected area diffraction pattern (SADP) shown in the inset. The presence of ω phase is confirmed by the presence of additional reflections along 1/3 and 2/3{112} diffraction vectors (or g vectors) [13,24]. This dark-field image was recorded using one of the 1/3{112}β reflections corresponding to the ω phase. APT studies were also performed on the β-solutionized sample. The raw ion maps for V and Al, shown in Fig. 1 (b-c), do not exhibit any discernible pockets devoid or enriched in any of the solute atoms, indicating a near-random distribution. Additionally, frequency distribution analysis was performed on the raw data of the Ti ions and compared to a theoretical binomial distribution (representing a random distribution). It can be seen that both the distributions are nearly identical. APT analysis could not detect any statistically relevant composition partitioning in the β-solutionized condition, leading to the conclusion that these quenched-in precipitates are athermal ω precipitates which inherit the composition of the parent β matrix.

Following the β-solutionizing, the samples were annealed at 330°C for times ranging from 0-150 hours to develop isothermal ω precipitates. Subsequently, specimens were annealed within the α + β phase field at 600 °C for 1H to promote α precipitation, as schematically shown in Fig. 2(a). The corresponding microstructures are shown in Fig. 2(b–f). The scale of distribution of the α precipitates is substantially more refined in the case of Fig. 2(c–f), as compared to Fig. 2(b) which appears to be very similar to that formed by high temperature duplex-aging

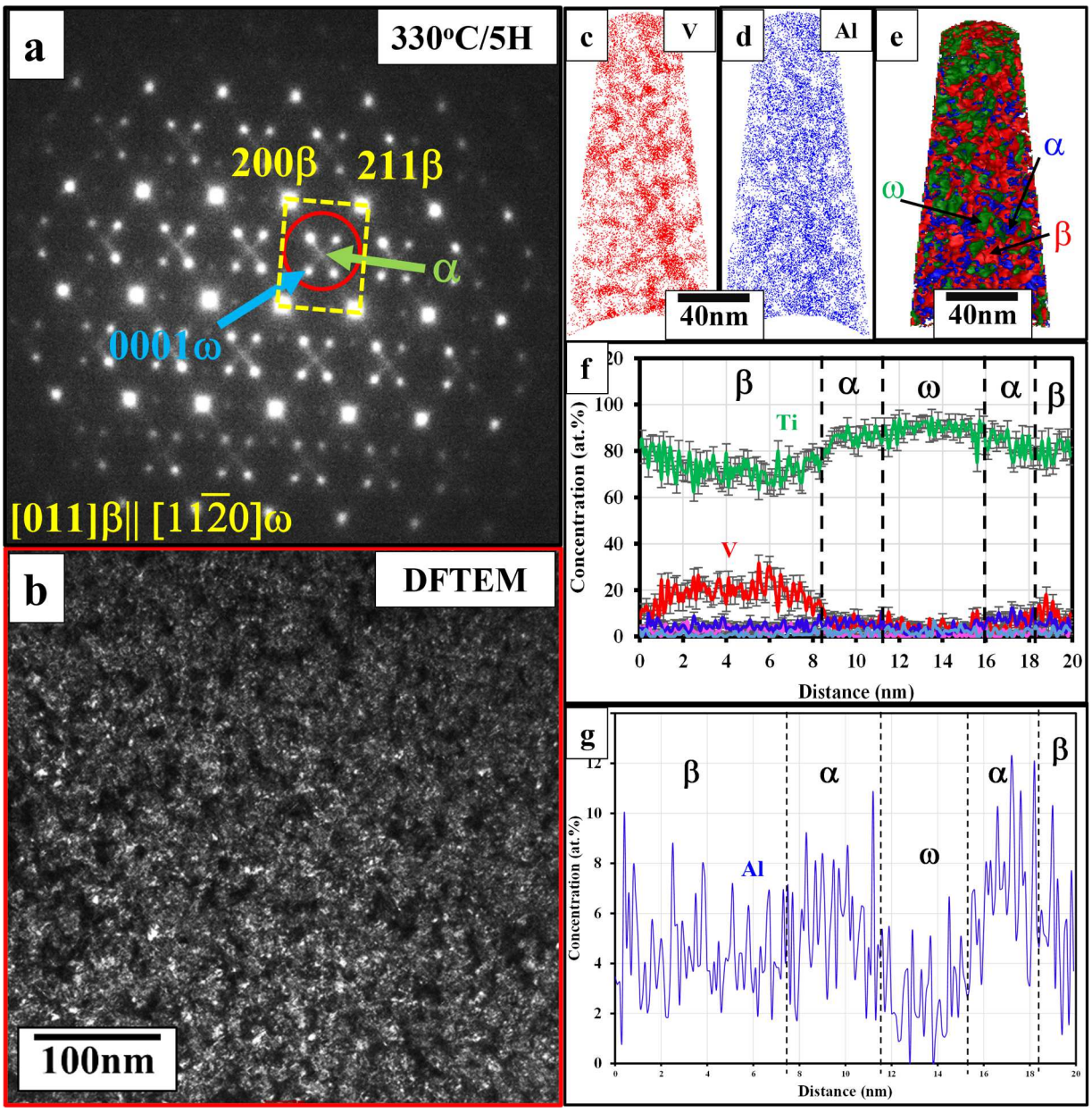

Fig. 3. 330C/5H sample: (a) SADP recorded along [110]β, showing ω reflections and early stage α reflection. (b)DFTEM showing ω precipitates, inset shows α precipitates, (c,d) elemental maps of the major elements V, Al show depletion. (e) proxigram shows clear evidence of β,ω,α. (f) compositional difference between β,ω, and α obtained via proxigram analysis. (g) Al partitioning between β,ω, and α.

treatments. The fine-scale α precipitation observed in the case of Fig. 2 (c–f) can presumably be attributed to the effect of prior isothermal ω precipitation during the first step of annealing at 330 °C. Such ω-assisted fine-scale α precipitation has been previously reported in other β-Ti alloys [1,10,19]. The samples aged for longer time periods at 330°C, not only exhibit a finer precipitate size, but also a higher number density. From this, it is evident that annealing below the ω transus plays an important role on the fine scale α precipitation in this alloy. Detailed microstructural analysis using TEM and APT was carried out on the samples annealed only at 330°C to decipher the specific role of the ω precipitates on α precipitation.

Fig. 3 shows the microstructure of the sample which was annealed at 330°C/5H. The SADP recorded along one of the <011>β zone axis, from this sample is shown in Fig. 3(b). In addition to the fundamental β (BCC) reflections, this SADP also shows additional sharp intense reflections at the 1/3 and 2/3{112}β locations, which can be attributed to the ω phase [9,24]. Additionally, a low intensity faint reflection can be seen at the 1/2{112}β locations, which has been previously attributed to early stages of formation of α precipitates [19]. The orientation relationships for β/ω and β/α are as follows [9]:

{111}β ||{0001}ω and <10-1>β ||<11-20>ω
{110}β || {0001}α and <1-11> β || [11–20]α

The DFTEM image shown in Fig. 3(b) has been recorded from a set of four adjacent ω reflections and one α reflection in the center, as marked by the circle in Fig. 3(a). This dark-field image shows the presence of fine scale ω precipitates exhibiting a largely spherical morphology, uniformly distributed throughout the microstructure. Additionally, a few lath-like or plate-like early stage α precipitates are also highlighted in this dark-field image, and a set of these are shown in the magnified view shown as an inset in Fig. 3(b). Compositional partitioning between these

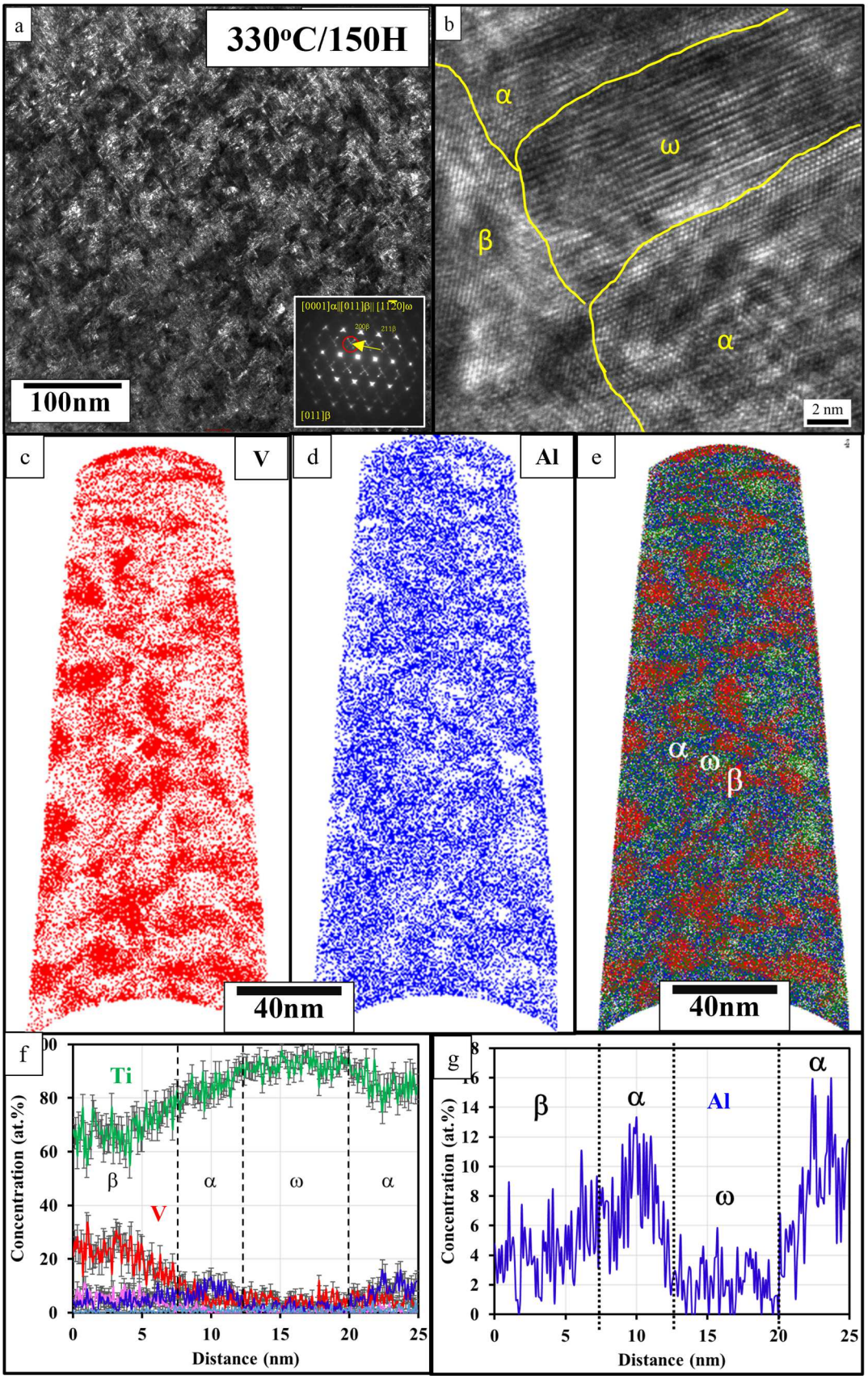

Fig. 4. 330C/150H sample (a) DFTEM showing ω and α precipitates, inset shows SADP along [110]β,(b)HRTEM image showing interfaces along β,ω,α phases (c, d) elemental maps of the major elements V, Al show depletion. (e) proxigram shows clear evidence of β, ω,α. (f) compositional difference between β,ω, and α obtained via proxigram analysis. (g) Al partitioning between β, ω, and α.

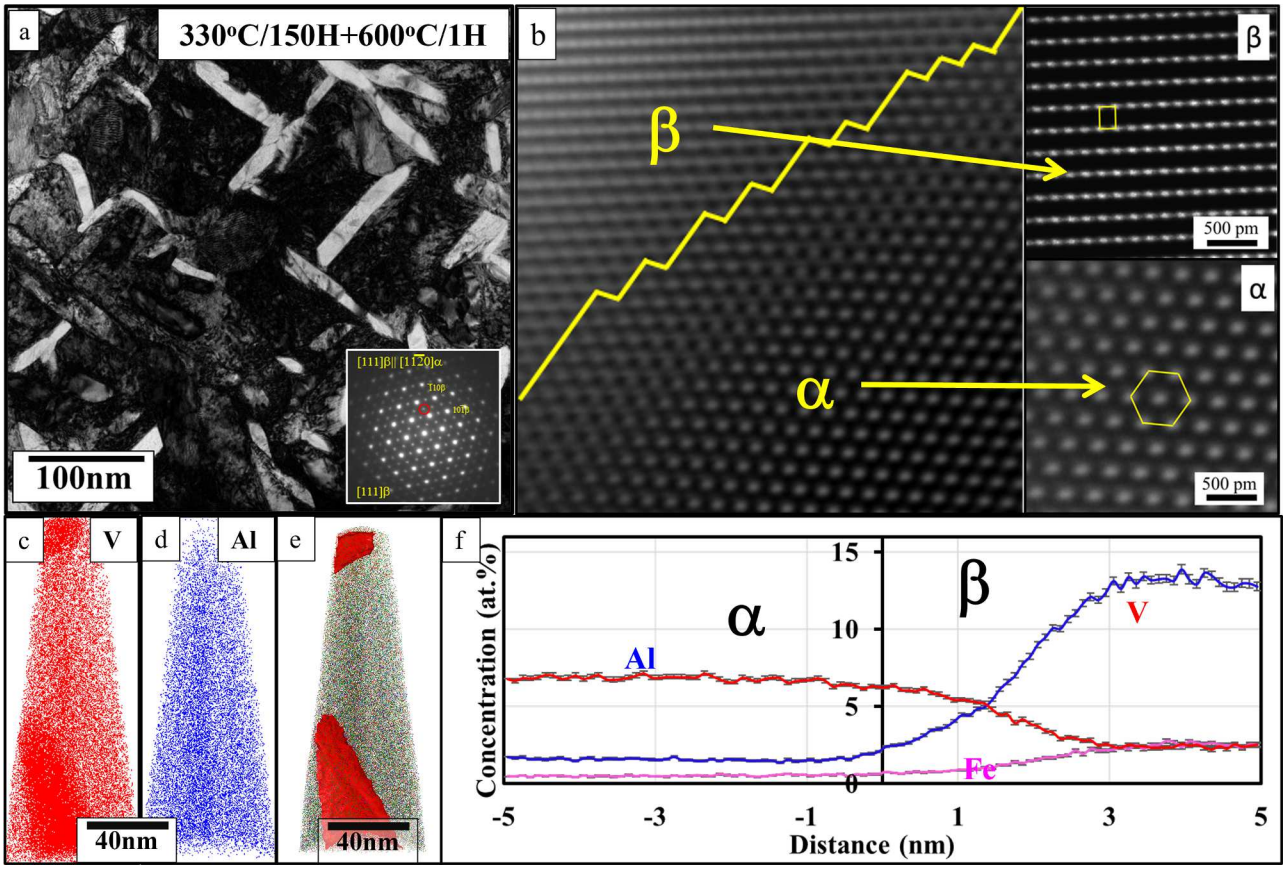

Fig. 5. 330C/150H+600C/1H sample (a) DFTEM showing α precipitates, inset shows SADP along [111]β,(b)HRTEM image showing interfaces along β,α phases (c, d) elemental maps of the major elements V, Al show depletion (e) proxigram shows clear evidence of β,α. (f) compositional difference between β and α obtained via proxigram analysis.

phases, after 330°C/5H annealing, was examined using APT. The raw ion maps of the reconstructed APT tips showed regions depleted in V and Al, in Fig. 3(c) and (d) respectively. These solute depleted regions can be identified as ω precipitates. Proximity histograms shown in Fig. 3(f) reveal the partitioning of elements between the β, ω, and α phases. Of particular interest here is the partitioning of Al, which has been highlighted in Fig. 3(g). While α precipitates reject β stabilizers like V and Fe, and are enriched in α stabilizers, such as Al, the ω precipitates reject all these three solute elements. A closer inspection of the Al proxigram (Fig. 3(g)), reveals that Al is rejected by both β and ω phases and piles up at the ω/β interface. Combination of the TEM and APT results indicates that there are very early stages of fine scale α precipitates forming after 5H annealing at 330°C, presumably in the regions exhibiting Al pile-up at the ω/β interface.

The second 330°C annealed sample investigated in detail was the one annealed for the maximum time of 150H. The microstructure of this sample is shown in Fig. 4. The <011>β SADP shows ω reflections at 1/3 and 2/3{112}β, and a sharp reflection at the 1/2{112}β location (arrow in Fig. 4(a)), indicating the presence of α phase. A DFTEM image revealed that these ω precipitates have coarsened. Additionally, extremely fine lath-like or plate-like α precipitates were also observed alongside the ω precipitates. A high-resolution TEM image shown in Fig. 4(b) clearly exhibits the co-existence of β, ω, and α phases in this condition with well-defined α/β, α/ω, and ω/β interfaces. The solute content of β, ω, and α phases was further investigated using APT in the present case. Similar to the 5H condition the raw ion maps of V and Al after 330°C/150H of annealing, indicated that the ω and α precipitates are solute depleted pockets. Superimposed Ti, V, and Al isosurfaces revealed a sharper Al pile-up adjacent to ω precipitates. Based on the high-resolution TEM analysis, this Al pile up can be attributed to the α precipitates. Proximity histograms presented in Fig. 4(f), show the partitioning of elements between the β, ω, and α phases. The partitioning of Al has been highlighted in Fig. 4(g). The depletion of Al in ω and β phases, while being enriched in α phase is noted.

Since the sample annealed at 330 °C/150H followed by annealing at 600°C/1H showed the finest scale of α precipitates, further analysis was carried out on this condition, and the results are shown in Fig. 5. The SADP, recorded along [111]β (shown as an inset in Fig. 5(a)), contains additional reflections at the 1/2{011}β locations corresponding to the α phase. The DFTEM image (Fig. 5(a)) recorded from one of these α reflections, reveals well-developed fine scale α precipitates ~ 80 – 150 mm in length. The high-resolution TEM image, shown in Fig. 5(b), reveals the atomic structure of the α/β interface recorded along the [0001]α || <011>β viewing axis. Characteristic atomic scale ledges or steps are clearly visible along this interface, similar to those reported in case other metastable β Ti alloys, such as Ti-5553 [1]. The atomic structure within the BCC β matrix, viewed along the [111] direction and the atomic structure of the HCP α phase, viewed along the [0001] direction are also shown in the same figure. Detailed APT analysis has been carried out and the results are shown in Fig. 5(c-f). As expected, Al strongly

Table 1
Al composition as a function of temperature in ω,β,α phases

Condition	**α** (Al at%)	**β** (Al at%)	**ω** (Al at%)
β soln	-	5.25	5.25
330°C/5H	10	4.71	2.16
330°C/150H	11.4	2.94	0.26
330°C/150H + 600°C/1H	7.1	2.3	-
Pandat Calculations (330°C)	6.0	2.5	
Pandat Calculations (600°C)	6.94	2.50	-

partitions to the α phase while V and Fe, being β stabilizers, strongly partition to the β-matrix.

The experimental results presented in this paper lead to novel insights into the nucleation mechanism of fine scale α precipitates in a commercially available β-Ti alloy, Ti-10V-2Fe-3Al. With an increase in the aging time below the ω solvus, there is a continuous increase in the volume fraction and the size of the ω precipitates. This is accompanied by a rejection of Al, V, and Fe from the ω precipitates. Table 1 shows the change in the percentage of Al as a function of heat treatment in the three phases present, i.e. β, ω, and α. The β-soln condition which contains athermal ω, retained the composition of the original alloy. Upon subsequent heat treatments, with the coarsening of ω phase, Al is rejected out and can be seen to go from 5.25% to 2.16% to 0.26% in the 150H sample. The pile-up of Al near the ω/β interface (assumed to be early stage α) after 330°C/5H annealing, exhibits an Al content as high as 10 at%, which goes as high as 11.4 at% after annealing at the same temperature for 150H. This supersaturation potentially acts as a nucleation site for the formation of the fine scale α precipitates. In contrast, the Al content in the αprecipitates in the two-step annealed (330°C/150H + 600°C/1H) is close to 7 at%. Solution thermodynamic based Pandat calculations were carried out using the PanTi database [23], and the results are also shown in the same Table 1. At 330°C, the predicted equilibrium Al content in the α phase is ~ 6 at%, which is much lower than the experimentally observed 10 – 11.4 at% in the single-step annealed samples at 330°C. However, the predicted equilibrium Al content in the α phase at 600°C is ~ 6.9 at%, in excellent agreement with the experimentally observed Al content ~ 7.1 at% in the α precipitates after the two-step annealing (330°C/150H + 600°C/1H). Importantly, the Pandat computations do not take into account the presence of the metastable ω phase in case of the 330°C prediction. Combining these Pandat predictions with the APT measured phase compositions, leads to some novel insights into the Al redistribution during ω-assisted α nucleation in β-Ti alloys. The experimental APT results indicate that at temperatures below the ω solvus, there exists a β+ω+α three-phase metastable equilibrium with three different levels of Al in the three phases. At 330°C (150H annealed), this three-phase metastable equilibrium in case of Ti-10-2-3 results in Al contents of 2.9 at%, 0.3 at%, and 11.4 at%, in β, ω, and α, respectively. Since the Al content in ω is about a tenth of that within the β phase, the three-phase metastable equilibrium increases the Al content within the α phase to 11.4 at%, nearly double of the 6 at% Al predicted by Pandat, based on a β+α two-phase equilibrium at 330°C. However, when the sample is annealed at a higher temperature of 600°C (substantially above the ω solvus temperature), the β+α two-phase equilibrium is restored and consequently the experimentally measured Al content of ~7.1 at%, is in excellent agreement with the Pandat prediction of ~ 6.9 at% Al in the α phase.

Summarizing, this paper presents direct experimental evidence and quantitative determination of Al pile up at the ω/β interfaces of β-Ti alloys, leading to early stages of α precipitation. These fine scale α precipitates nucleate at the ω/β interfaces, and form ω/α and α/β interfaces. A novel β+ω+α three-phase metastable equilibrium results at low temperatures, with a substantially higher Al content within α precipitates, than predicted by solution thermodynamics (Pandat models).

Declaration of Competing Interest

The authors declare that they have no known competing financial interests or personal relationships that could have appeared to influence the work reported in this paper.

Acknowledgments

This research has been supported by the National Science Foundation (NSF), Division of Materials Research (DMR) under grants DMR-1905844 and DMR-1905835.

References

[1] S. Nag, R. Banerjee, R. Srinivasan, J.Y. Hwang, M. Harper, H.L. Fraser, ω-Assisted nucleation and growth of α precipitates in the Ti-5Al-5Mo-5V-3Cr-0.5Fe β titanium alloy, Acta Mater. 57 (7) (2009) 2136–2147, https://doi.org/10.1016/j.actamat.2009.01.007.

[2] T. Li, D. Kent, G. Sha, M.S. Dargusch, J.M. Cairney, The mechanism of ω-assisted α phase formation in near β-Ti alloys, Scr. Mater. 104 (2015) 75–78, https://doi.org/10.1016/J.SCRIPTAMAT.2015.04.007.

[3] K. Chou, E.A. Marquis, Oxygen effects on ω and α phase transformations in a metastable β Ti–Nb alloy, Acta Mater. 181 (2019) 367–376, https://doi.org/10.1016/J.ACTAMAT.2019.09.049.

[4] J. Šmilauerová, et al., Lamellae of α phase in a metastable β-Ti alloy studied by small-angle x-ray scattering, Mater. Charact. 196 (2023), https://doi.org/10.1016/j.matchar.2022.112615.

[5] Y. Zheng, R.E.A. Williams, J.M. Sosa, Y. Wang, R. Banerjee, H.L. Fraser, The role of the ω phase on the non-classical precipitation of the α phase in metastable β-titanium alloys, Scr. Mater. 111 (2016) 81–84, https://doi.org/10.1016/J.SCRIPTAMAT.2015.08.019.

[6] I. Weiss, S.L. Semiatin, Thermomechanical processing of beta titanium alloys—an overview, Mater. Sci. Eng.: A 243 (1–2) (1998) 46–65, https://doi.org/10.1016/S0921-5093(97)00783-1.

[7] S. Ankem, C.A. Greene, Recent developments in microstructure/property relationships of beta titanium alloys, Mater. Sci. Eng.: A 263 (2) (1999) 127–131, https://doi.org/10.1016/S0921-5093(98)01170-8.

[8] O.M. Ivasishin, P.E. Markovsky, Y.V. Matviychuk, S.L. Semiatin, C.H. Ward, S. Fox, A comparative study of the mechanical properties of high-strength β-titanium alloys, J. Alloys Compd. 457 (1–2) (2008) 296–309, https://doi.org/10.1016/J.JALLCOM.2007.03.070.

[9] D. Banerjee, J.C. Williams, Perspectives on Titanium Science and Technology, Acta Mater. 61 (3) (2013) 844–879, https://doi.org/10.1016/J.ACTAMAT.2012.10.043.

[10] S.A. Mantri, et al., Tuning the scale of α precipitates in β-titanium alloys for achieving high strength, Scr. Mater. 154 (2018) 139–144, https://doi.org/10.1016/J.SCRIPTAMAT.2018.05.040.

[11] D. De Fontaine, N.E. Paton, J.C. Williams, The omega phase transformation in titanium alloys as an example of displacement controlled reactions, Acta Metallur. 19 (11) (1971) 1153–1162, https://doi.org/10.1016/0001-6160(71)90047-2.

[12] Y. Ohmori, T. Ogo, K. Nakai, S. Kobayashi, Effects of ω-phase precipitation on β→α, α′′ transformations in a metastable β titanium alloy, Mater. Sci. Eng.: A 312 (1–2) (2001) 182–188, https://doi.org/10.1016/S0921-5093(00)01891-8.

[13] D. Choudhuri, et al., Coupled experimental and computational investigation of omega phase evolution in a high misfit titanium-vanadium alloy, Acta Mater. 130 (2017) 215–228, https://doi.org/10.1016/J.ACTAMAT.2017.03.047.

[14] P. Zháňal, et al., Evolution of ω phase during heating of metastable β titanium alloy Ti–15Mo, J. Mater. Sci. 53 (1) (2018) 837–845, https://doi.org/10.1007/s10853-017-1519-2.

[15] T. Ahmed, H.J. Rack, Phase transformations during cooling in α+β titanium alloys, Mater. Sci. Eng.: A 243 (1–2) (1998) 206–211, https://doi.org/10.1016/S0921-5093(97)00802-2.

[16] F. Prima, P. Vermaut, G. Texier, D. Ansel, T. Gloriant, Evidence of α-nanophase heterogeneous nucleation from ω particles in a β-metastable Ti-based alloy by high-resolution electron microscopy, Scr. Mater. 54 (4) (2006) 645–648, https://doi.org/10.1016/J.SCRIPTAMAT.2005.10.024.

[17] T. Li, et al., New insights into the phase transformations to isothermal ω and ω-assisted α in near β-Ti alloys, Acta Mater. 106 (2016) 353–366, https://doi.org/10.1016/J.ACTAMAT.2015.12.046.

[18] Y. Zheng, et al., The indirect influence of the ω phase on the degree of refinement of distributions of the α phase in metastable β-Titanium alloys, Acta Mater. 103 (2016) 165–173, https://doi.org/10.1016/J.ACTAMAT.2015.09.053.

[19] Y. Zheng, et al., Role of ω phase in the formation of extremely refined intragranular α precipitates in metastable β-titanium alloys, Acta Mater. 103 (2016) 850–858, https://doi.org/10.1016/J.ACTAMAT.2015.11.020.

[20] Y. Zheng, D. Choudhuri, T. Alam, R.E.A. Williams, R. Banerjee, H.L. Fraser, The role of cuboidal ω precipitates on α precipitation in a Ti-20V alloy, Scr. Mater. 123 (2016) 81–85, https://doi.org/10.1016/J.SCRIPTAMAT.2016.06.004.

[21] T.W. Duerig, J. Albrecht, D. Richter, P. Fischer, Formation and reversion of stress induced martensite in Ti-10V-2Fe-3Al, Acta Metallur. 30 (12) (1982) 2161–2172, https://doi.org/10.1016/0001-6160(82)90137-7.

[22] F. Sun, F. Prima, T. Gloriant, High-strength nanostructured Ti–12Mo alloy from ductile metastable beta state precursor, Mater. Sci. Eng.: A 527 (16–17) (2010) 4262–4269, https://doi.org/10.1016/J.MSEA.2010.03.044.

[23] S.L. Chen, et al., The PANDAT software package and its applications, Calphad 26 (2) (2002) 175–188, https://doi.org/10.1016/S0364-5916(02)00034-2.

[24] B.S. Hickman, The formation of omega phase in titanium and zirconium alloys: a review, J. Mater. Sci. 4 (6) (1969) 554–563, https://doi.org/10.1007/BF00550217.